Cancer Chemother Pharmacol (2010) 65:207–217
DOI 10.1007/s00280-009-1023-8

ORIGINAL ARTICLE

Mechanism-based receptor-binding model to describe the pharmacokinetic and pharmacodynamic of an anti-$\alpha_5\beta_1$ integrin monoclonal antibody (volociximab) in cancer patients

Chee M. Ng · S. Bai · C. H. Takimoto · M. T. Tang · A. W. Tolcher

Received: 7 December 2008 / Accepted: 29 April 2009 / Published online: 26 May 2009

Abstract
Purpose Volociximab is a chimeric IgG_4 that is being developed as a novel first-in-class anti-angiogenic, $\alpha_5\beta_1$ integrin inhibitor for the treatment of solid tumors. A mechanism-based pharmacokinetic (PK)/pharmacodynamic (PD) model was developed to investigate the dynamic interaction between volociximab concentrations and free monocyte $\alpha_5\beta_1$ integrin levels in cancer patients.
Methods Twenty-one cancer patients from six dose cohorts (0.5, 1.0, 2.5, 5.0, 10, and 15 mg/kg) were included in the analysis. The fully integrated receptor-binding PK/PD model was developed and fit simultaneously to the PK/PD data. A Monte-Carlo parametric expectation-maximization method implement in S-ADAPT program was used to obtain estimates of population parameters and inter- and intra-subject variability.
Results The PK/PD time profiles were well described by the model and the parameters were estimated with good precision. The model was used to simulate PK/PD time profiles for multiple dose regimens at various dose levels, and the results suggested that the monocyte $\alpha_5\beta_1$ integrin binding was saturated ($\leq$5% free) at week 16 in the majority of patients treated with volociximab doses $\geq$10 mg/kg IV every 2 weeks.
Conclusions The developed model is useful for anticipating the drug exposures and extent of volociximab binding to peripheral monocyte $\alpha_5\beta_1$ integrin in untested regimens and for optimizing the design of future clinical trials.

Keywords Pharmacodynamic · Monoclonal antibody · Pharmacokinetic · Volociximab · Integrin · Model · Phase I

C. M. Ng (✉)
Cancer Therapy and Research Center,
Institute for Drug Development, The University of Texas Health Science Center at San Antonio,
7979 Wurzbach Road, San Antonio, TX 78229, USA
e-mail: ng.cheem@yahoo.com

S. Bai
Genentech, South San Francisco, CA, USA

C. H. Takimoto · A. W. Tolcher
South Texas Accelerated Research Therapeutics (START), San Antonio, TX, USA

M. T. Tang
Facet Biotech, Corp, Redwood City, CA, USA

Introduction

Angiogenesis is involved in the pathogenesis of a number of clinical conditions, including malignant tumor growth and neovascular age-related macular degeneration [11, 12, 26]. Angiogenesis is a complex process mediated by growth factors, such as vascular-endothelial growth factor (VEGF), and proteins, such as integrins and matrix metalloproteases [3, 24]. Although the role of VEGF in directing angiogenesis is well documented [10], recent evidence suggests that integrins are also important in the angiogenesis process [5]. Although the growth factors are required to stimulate new blood vessel growth, the interaction between the cell surface integrins and the extracellular matrix (ECM) is important in regulating endothelial cell survival, proliferation, and motility during new blood vessel growth [4, 5].

Integrins are heterodimeric adhesion proteins consisting of α and β subunits [16]. Specific dimeric pairs of integrin subunits show tissue specificity; each α and β dimer has

unique signaling properties triggered by binding to specific ECM ligands [16]. Integrin $\alpha_5\beta_1$ is expressed at low levels on mature vasculature, but is upregulated during angiogenesis in experimental model system [18]. Interaction between the integrin $\alpha_5\beta_1$ and its ligand, fibronectin following growth factor stimulation is important in vascular development [13, 15]. Antagonists that specifically block the binding of fibronectin to $\alpha_5\beta_1$ integrin inhibit endothelial cell survival and proliferation in vitro and in vivo, even when other integrins are present that can bind to the ECM [15]. Furthermore, inhibitors of $\alpha_5\beta_1$ integrin and fibronectin block angiogenesis in experimental animal model [17].

Volociximab is a high affinity, chimeric IgG_4 monoclonal antibody under development as an anti-angiogenic, $\alpha_5\beta_1$ integrin inhibitor for the treatment of solid tumors. Unlike current anti-angiogenic pathway inhibitors, such as the anti-VEGF antibody bevacizumab, volociximab inhibits endothelial cell proliferation downstream of growth factor stimulation and it is the first anti-$\alpha_5\beta_1$ monoclonal antibody to enter clinical trials. In a Phase I, multicenter, open label, dose-escalation study, patients with tumors unresponsive to standard therapies were treated with volociximab at doses ranging from 0.5 to 15 mg/kg [23]. The occupancy of $\alpha_5\beta_1$ receptors on peripheral monocytes by volociximab was assessed as a potential biomarker. Volociximab was well tolerated and no dose-limiting toxicity was observed. Volociximab kinetics was not dose proportional over the dose range examined, consistent with nonlinear pharmacokinetics. Mean antibody clearance decreased from 141.6 mL/h at 0.5 mg/kg to 9.7 mL/h at 15 mg/kg [23]. The nonlinear PK of the volociximab may be explained by its saturable binding to $\alpha_5\beta_1$ integrin in tissues. Volociximab binds and saturates $\alpha_5\beta_1$ integrins on circulating monocytes and these receptors were fully saturated for the entire treatment period in patients treated at dose levels greater than 10 mg/kg dosed weekly. Currently, volociximab has been tested in Phase II cancer patients with various tumor types, including melanoma, pancreatic, and renal cell cancer [6, 9, 27]. The objective of this modeling effort is to develop a mechanism-based population PK/PD model to investigate the nature of nonlinear pharmacokinetics of volociximab and to increase our understanding of volociximab interactions with $\alpha_5\beta_1$ integrins in cancer patients in the Phase I study.

Methods

Antibody

Volociximab is a high affinity, chimeric (82% human, 18% murine) IgG_4 monoclonal antibody that specifically binds to $\alpha_5\beta_1$ integrin, a cell-surface receptor for fibronectin. It is composed of the variable region of the murine antibody, IIA1, including the complementary determining region (CDR) region directed against human $\alpha_5\beta_1$ integrin, and the constant region from human IgG_4 heavy and kappa light chains. The molecular weight of volociximab is 146 kDa and it is supplied as a sterile, colorless, preservative-free solution for IV use. For this study, 10 mL single-use vials containing 100 mg of volociximab at a concentration of 10 mg/mL in 25 mM sodium citrate, 150 mM sodium chloride, and 0.05% polysorbate 80 at a pH of 6.5 were used.

Patients

The study was a Phase I, multicenter, open label, single arm, dose-escalation trial to investigate the safety, tolerability, and PK of volociximab in adult subjects with solid tumors unresponsive to standard therapies [23]. A total of 21 subjects were enrolled into six dose cohorts: 0.5 ($n = 1$), 1 ($n = 2$), 2.5 ($n = 3$), 5 ($n = 3$), 10 ($n = 6$), and 15 ($n = 6$) mg/kg. Each subject received five 1 h IV infusions of volociximab with the first and second doses separated by a 2-week period. The remaining three doses were given weekly on study days 22, 29, and 36 followed by a 45-day observation period. Pharmacokinetic samples were collected at the following times; pre-dose, and 1, 4, 24, 48, and 168 h after the start of the infusion on day 1. On days 15, 22, 29, and 36, samples were collected before the next dose, and 1 and 4 h after dosing. Additional samples were collected on days 38, 43, and 81 during the evaluation period after the last dose. To determine the saturation of $\alpha_5\beta_1$ integrin binding by volociximab on circulating monocytes as a PD marker, samples of peripheral blood were collected before dosing on days 1, 2, 8, and 43. Serum samples for anti-drug antibodies (ADAb) were obtained before treatment, prior to the second dose, and at the planned study exit on day 81, 45 days after the last dose of volociximab. In addition, selected serum PK samples were used for testing ADAb if the day 81 sample was not available.

Analytical methods

Volociximab concentrations were determined using a validated enzyme-linked immunosorbent assay (ELISA). Briefly, AAB1/B2Fc, a fusion protein containing the human $\alpha_5\beta_1$ heterodimer and human IgG_1 Fc domain, was used as the capture reagent for volociximab. Samples were incubated on AAB1/B2Fc-coated plates and detection was accomplished using a biotin-conjugated mouse anti-human IgG_4 with a streptavidin-HRP conjugate. Tetramethylbenzidine was used as a substrate and absorbance was read

at 650 nm. The validated quantitative range of the assay was 100–1,500 ng/mL in human serum.

The saturation of $\alpha_5\beta_1$ sites on peripheral monocytes was determined by flow cytometry using CD14 antibodies to identify monocytes and by the addition of labeled anti-human IgG_4 to quantitate bound volociximab on the cell surface. Unoccupied $\alpha_5\beta_1$ integrin sites were detected by the addition of labeled murine anti-human $\alpha_5\beta_1$ antibody (IIA1).

The immunogenicity of volociximab was first evaluated using a double-antigen bridging ELISA (screening) assay. Briefly, anti-volociximab antibodies were captured on microtiter plates coated with volociximab and were quantitated using biotinylated volociximab and streptavidin-HRP. Human serum containing murine anti-volociximab antibodies (idiotype specific, ADAb) at different concentrations were used as the positive control and to generate a calibration curve. The quantitative range of the assay was 5–500 ng/mL anti-idiotype equivalents. Samples testing positive for ADAb in the screening ELISA were further evaluated in a validated confirmatory assay. In the confirmatory assay, samples were preincubated with an excess of volociximab before adding the solution to volociximab-coated plates. Similar to the screening ELISA, bound antibody was detected using biotinylated volociximab with streptavidin-HRP and visualized with tetramethylbenzidine. Confirmed ADAb-positive serum samples were further evaluated in a neutralizing antibody (NAb) assay. Samples were preincubated with phycoerythrin-labeled volociximab prior to incubation with U937 cells that highly expressed the $\alpha_5\beta_1$ integrin target on their surface. Cells were fixed and analyzed by flow cytometry to measure the mean fluorescence intensity (MFI) of bound phycoerythrin-volociximab. Reduced MFI for bound phycoerythrin-volociximab indicates a NAb activity in the tested samples.

Model development and data analysis

A receptor-mediated PK/PD model that characterized the relationship between serum volociximab concentration and percent-free monocyte $\alpha_5\beta_1$ integrin expression was developed (Fig. 1) and fitted simultaneously to both PK and PD datasets. Elimination of volociximab in the central plasma compartment was assumed to be via both nonspecific (CL) and receptor-mediated specific clearance pathways. The receptor-mediated clearance pathway was modeled as an interaction between drug (X_c) and free monocyte $\alpha_5\beta_1$ integrin (R_f) to form a drug–receptor complex (X_R) via reversible binding with a association/dissociation rate constant (K_{on} and K_{off}), with subsequent turnover of the drug–receptor complex (K_{int}). A tissue compartment with linear first-order distribution processes (CL_d) was used to account for nonspecific drug binding and distribution.

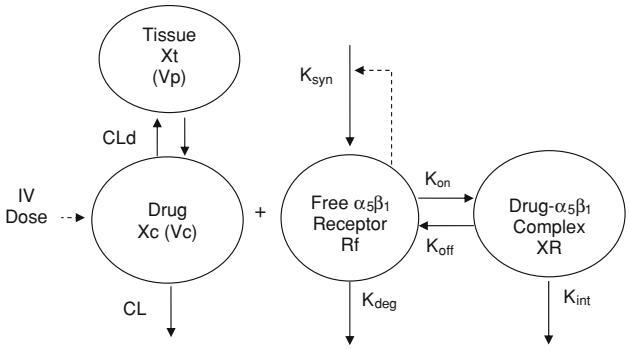

Fig. 1 Schematic representation of mechanism-based PK/PD model of volociximab

The differential equations describing the volociximab PK/PD model (Fig. 1) are as follows:

$$\frac{dX_c}{dt} = \left(\frac{CL}{V_c} + \frac{CL_d}{V_c}\right)X_c + \frac{CL_d}{V_p}X_t - \left(K_{on}\frac{X_c}{V_c}Rf - K_{off} \times X_R\right)V_c \quad (1)$$

$$\frac{dX_t}{dt} = \frac{CL_d}{V_c}X_c - \frac{CL_d}{V_p}X_t \quad (2)$$

$$\frac{dR_f}{dt} = K_{syn}\left(\frac{Rf}{Base}\right)^{\theta} - K_{deg}R_f - K_{on}\frac{X_c}{V_c}R_f + K_{off}X_R \quad (3)$$

$$\frac{dX_R}{dt} = K_{on}\frac{X_c}{V_c}R_f - K_{off}X_R - K_{int}X_R \quad (4)$$

In this model, X_c and X_t are the amount of free volociximab in central and tissue compartments and R_f and X_R are the free monocyte $\alpha_5\beta_1$ receptor and volociximab–$\alpha_5\beta_1$ complex concentrations, respectively. The inter-compartmental clearance is CL_d and V_p is the volume of distribution of the peripheral compartment. The clearance of nonspecific IgG_4 pathway is CL and V_c is the volume of distribution of free volociximab in the central compartment. The zero-order synthesis rate and first-order elimination rate constants of free $\alpha_5\beta_1$ receptor are K_{syn} and K_{deg}, respectively, while K_{on} and K_{off} are the association and dissociation rate constants for volociximab-$\alpha_5\beta_1$ binding. K_{int} is the first-order internalization/degradation rate constant of the $\alpha_5\beta_1$–receptor complex and Base is the baseline concentration for the $\alpha_5\beta_1$ receptor before volociximab treatment. Lastly, θ is the coefficient for the negative feedback loop for the $\alpha_5\beta_1$ receptor, which is similar to the feedback parameter used in the chemotherapy-induced neutropenia model [14]. In the absence of volociximab, the free and total $\alpha_5\beta_1$ receptor concentrations were equal to the baseline $\alpha_5\beta_1$ receptor concentration. Owing to the limited PK/PD data used in the analysis, the goal was to develop a mechanism-based model that was supported by the data and to minimize the number of parameters to be estimated. Hence, it was assumed in the modeling that $K_{int} = K_{deg}$.

This model was fitted simultaneously to the individual volociximab concentration data and the percent-free monocyte $\alpha_5\beta_1$ receptor data using the Monte-Carlo expectation-maximization (MCPEM) algorithm implemented in the S-ADAPT II program, an augmented version of ADAPT II with population analysis capabilities [1, 7]. The inter-subject variability was assumed to be log-normally distributed and was fitted using an exponential model. During the model development, several residual errors models (proportional, additive, mixed proportional and additive, and poisson error) were tested. Based on the results from the likelihood ratio test, parameter estimates and visual inspection of the diagnostic plots, proportional error, and Poisson error models were selected to describe the residual variability of the PK and PD models, respectively. The serum volociximab concentrations below 0.1 μg/ml (level of quantification) were handled as fixed point censored observations and the maximum likelihood was used to fit the model to the censored observations [2]. In this case, the likelihood for all the data is maximized with respect to the model parameters and the likelihood for a censored concentration in particular was taken to be the likelihood that the censored observation is truly below the level of quantification. The model was then used to fit the PK/PD data simultaneously. Differences in objective function of greater than 10.83 for 1 degree of freedom, corresponding to a significance level of $P < 0.001$, were used to discriminate two nested hierarchical models. This stringent criterion was used because of the inherent random noise associated with the Monte-Carlo sampling technique employed in the MCPEM algorithm. A series of diagnostic tests were implemented to examine the MCPEM model convergence. First, the population mean parameters and inter-subject variances of the last five iterations are averaged and compared with the average of those parameters obtained from the previous five iterations. If the fractional difference from each other is <0.01, the population analysis is terminated. If they differ from each other by more than 0.01, then the last ten iterations of the population mean parameters and inter-subject variances are examined using linear regression analysis. A Bonferroni method using the following equation was used to adjust the P value of the linear regression analysis for multiple parameters:

$$\alpha_B = \frac{\alpha}{C} \tag{5}$$

In this case, α_B, α, and C were the Bonferroni-adjusted P values, preset P value (set at 0.05), and numbers of tested parameters, respectively. If the changes in all tested parameters across iterations are not statistically different from zero, then model convergence is assumed.

The ability of the final PK/PD model to describe the observed data was investigated using a visual predictive check and simplified numerical predictive model checking method [20]. The final model, including fixed-effect and inter-subject random effect parameters, was used to simulate 500 replications of the observed data set. The simulated data were sorted by observation times and patients, and the 97.5th, 50th (median), and 2.5th quantile of the pooled simulated data were calculated for each observed time point for individual subjects. The percent of observed data that fell within the boundaries of the 97.5th and 2.5th quantile (95% confidence interval) and below or above 50th quantile of the pooled simulated data were determined. When the model simulation results matched perfectly to the distribution of the observed data, 95% of the observed data should be located within the 95% confidence interval of the simulated data, and 50% of the observed data should be below or above the 50th quantile of the pooled simulated data. The model was considered adequately described the distribution of the observed data if the percent of observed data was ±5% within the 95% confidence interval and 50th quantile of the pooled simulated data.

Volociximab has time-linear kinetic/dynamic characteristics and remains constants after multiple dose treatment in cancer patients, therefore, the final model was used to simulate PK/PD profiles generated by different multiple dose regimens.

Results

In this first-in human trial of volociximab, pharmacokinetics, and pharmacodynamics were investigated after the administration of multiple intravenous doses (0.5, 1.0, 2.5, 5.0, 10, and 15 mg/kg) in solid tumor patients unresponsive to standard therapies. Twenty-one subjects (8 females and 13 males) were included in the analysis. The summary of patient demographics is listed in Table 1. Initially, a total of 552 PK and PD samples were collected from study subjects. However, three subjects (1 in the 0.5 mg/kg group and 2 in the 1 mg/kg group) tested positive for ADAb and neutralizing antibodies and, therefore, 50 PK/PD blood samples following the second and subsequent volociximab doses from these subjects were excluded from analysis and model development. The final analysis dataset consisted of a total of 502 PK/PD samples. The dose-normalized mean volociximab concentration–time plot after first dose is shown in Fig. 2.

The lack of superimposition of dose-normalized volociximab concentrations suggests the nonlinearity of volociximab pharmacokinetics over this dose range in cancer patients. At dose levels higher than 5 mg/kg, monocyte $\alpha_5\beta_1$ levels were saturated in the presence of volociximab. Figure 3a–d are representative plots of pharmacokinetic

Table 1 Summary of subject demographic characteristics

	Volociximab dose group					
	0.5 mg/kg ($n = 1$)	1 mg/kg ($n = 2$)	2.5 mg/kg ($n = 3$)	5 mg/kg ($n = 3$)	10 mg/kg ($n = 6$)	15 mg/kg ($n = 6$)
Age (years)	55.0	31.5 (29–34)	60.7 (57–64)	60.7 (57–67)	61.8 (40–81)	41.7 (39–43)
Weight (kg)	71.0	55.5 (48–63)	79.7 (70–92.6)	81.1 (67.2–91.8)	69.9 (52.3–93.3)	90.8 (84–99)
Gender						
Male	1	1	1	3	2	5
Female	0	1	2	0	4	1
Race						
White	0	1	1	0	1	1
Others	1	1	2	3	5	5

Values indicated mean (range)

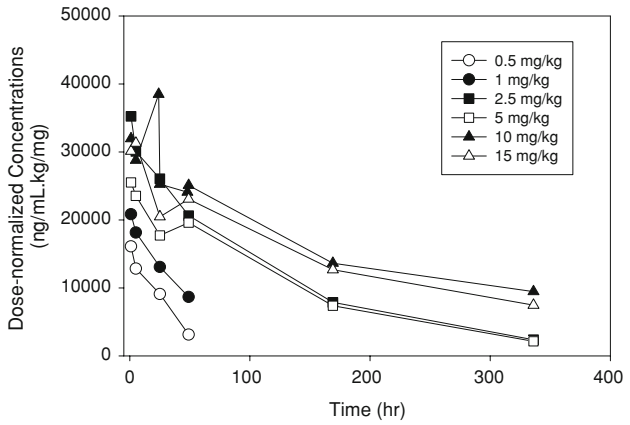

Fig. 2 Dose-normalized mean concentrations–time plot

and pharmacodynamic-time profiles and model predictions for patients in the 1.0, 2.5, 10, and 15 mg/kg dose groups, respectively. The majority of the free monocyte $\alpha_5\beta_1$ integrin was saturated at volociximab concentrations above 10 μg/mL. The free $\alpha_5\beta_1$ integrin gradually recovered to baseline level as the drug concentrations dropped below the assay limit of quantitation (Fig. 3a, b). The percent-free $\alpha_5\beta_1$ integrin on circulating monocytes returned to baseline before the second dose in patients treated at low-dose levels (Fig. 3a, b); however, integrin binding sites were saturated for the entire dosing period in the 10 and 15 mg/kg dose groups (Fig. 3c, d), indicating that the volociximab saturated monocyte $\alpha_5\beta_1$ integrins in a dose- and concentration-dependent manner.

A fully integrated mechanism-based receptor-binding PK/PD model was developed to describe the volociximab and percent-free monocyte $\alpha_5\beta_1$-time profiles in cancer patients (Fig. 1). The nonlinear pharmacokinetics of volociximab was assumed to be due to saturable binding of drug to $\alpha_5\beta_1$ integrins. The final model reasonably predicted the observed serum volociximab concentrations and monocyte $\alpha_5\beta_1$ integrin binding over time. Figure 4a includes individual predicted versus observed serum volociximab concentrations and monocyte $\alpha_5\beta_1$ integrin data for all patients. Generally, there was a good agreement between the predicted and observed individual data, and the diagnostic plots (Fig. 4a–d) of the final model identified no systematic bias. Representative plots of observed and model predicted serum volociximab concentrations and percent-free monocyte $\alpha_5\beta_1$ receptor levels in four subjects receiving different volociximab doses are shown in Fig. 3a–d. These plots further demonstrated that the final model reasonably described the data.

The estimated final PK/PD model parameters are presented in Table 2. The typical nonspecific clearance (CL) was 0.0544 mL/h/kg. The volume of distribution of central compartment (V_c 34.0 mL/kg) approximates plasma volume, as is expected for a high-molecular weight protein. The typical turnover rate of the free $\alpha_5\beta_1$ receptor (K_{deg}) is 0.00544 h^{-1}, which corresponds to a half-life of about 127 h or 5.3 days. The estimated equilibrium dissociation constant (K_d) for $\alpha5\beta1$-volociximab complex calculated as the ratio of K_{off} to K_{on}, was estimated to be 0.065 nM, indicating a high-affinity of the antibody for the monocyte $\alpha_5\beta_1$ integrin. The power coefficient (θ) for the negative feedback mechanism of the $\alpha_5\beta_1$ receptor synthesis was 0.590. The final PK/PD and inter- and intra-subject variability parameters for volociximab were estimated with good precision, with percent standard error of all of the parameter estimates <44%.

Figure 5 display the visual predictive performance of the final PK/PD model for patients who received a dose of 15 mg/kg, which indicated that the model adequately described the time course of volociximab and its effects on monocyte $\alpha_5\beta_1$ receptor. In addition, a simplified numerical model predictive check was used to examine the ability of the final model to describe the observed data. The final model was used to simulate 500 replications of the

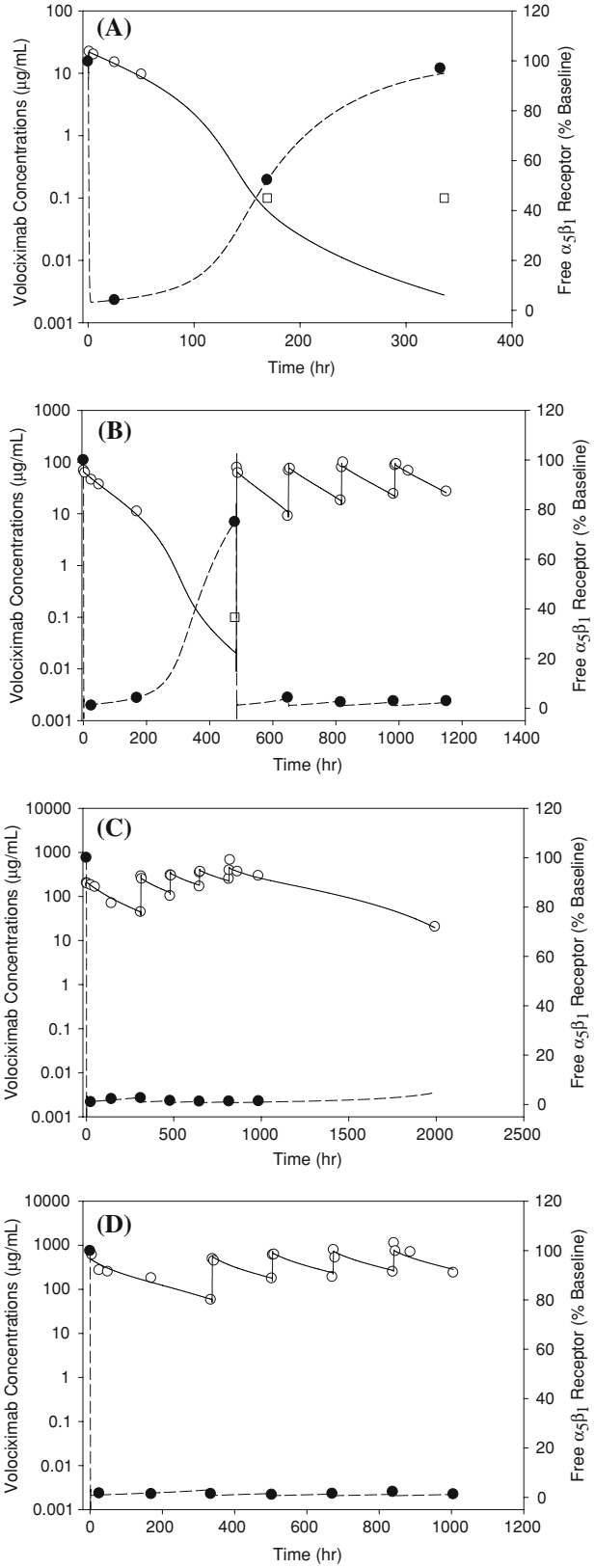

◀ **Fig. 3** Individual pharmacokinetic and pharmacodynamic-time profiles and model prediction from patients who received a dose of **a** 1 mg/kg, **b** 2.5 mg/kg, **c** 10 mg/kg, or **d** 15 mg/kg. *Open circle* observed volociximab concentration, *open square* observed volociximab concentrations below assay quantitative limit, *solid circle*, observed free $\alpha_5\beta_1$ receptor level, *solid line* model predicted volociximab concentrations, *dotted line* model predicted free $\alpha_5\beta_1$ receptor level

observed volociximab concentration dataset. The percent of observed data within the 95% quantile range, below the 50th quantile (median), and above the 50th quantile of the pooled simulated data were 95.3, 49.7, and 50.3%, respectively (Table 3). In a subgroup analysis, the percent of observed serum volociximab concentrations and percent-free $\alpha_5\beta_1$ receptor within the 95% quantile range of the pooled simulated data was 95.4 and 95.2%, respectively. Overall, these results suggest that the final PK/PD model was able to describe and predict the distribution of the data quite well.

The final PK/PD model was then used to simulate the data in examining the percent-free monocyte $\alpha_5\beta_1$ integrin response for various volociximab dosing regimens. The percent-free monocyte $\alpha_5\beta_1$ receptor profiles on week 16 from 1,000 simulated subjects were obtained for doses of 1, 2, 5, 10, 12.5 and 15 mg/kg IV infused over 1 h every 2 weeks. Figure 6a demonstrates the distribution of the percent-free monocyte $\alpha_5\beta_1$ receptors for simulated subjects after different dosing regimens of volociximab. These data suggest that volociximab doses of greater than 5 mg/kg every 2 weeks were necessary to saturate the monocyte $\alpha_5\beta_1$ integrin sites in a majority of subjects. In a further analysis, the relationship between volociximab dose and the percent-free monocyte $\alpha_5\beta_1$ integrin sites was constructed and is shown in Fig. 6b. The percentage of simulated subjects who achieved percent-free monocyte $\alpha_5\beta_1$ integrin levels $\leq$10% on week 16 were 10.6, 43.6, 86.4, 97.7, 97.3, 98.6, and 99.4% at volociximab doses of 1, 2, 5, 10, 12.5, 15, and 20 mg/kg, respectively. The percentage of simulated subjects who achieved free monocyte $\alpha_5\beta_1$ integrin responses $\leq$5% were 3.2, 23.4, 71.0, 93.2, 94.0, 98.6, and 99.4% for 1, 2, 5, 10, 12.5, 15, and 20 mg/kg dose levels, respectively. For the volociximab doses administered at 1, 2, 5, 10, 12.5, 15, and 20 mg/kg every 2 weeks, the percents of simulated subjects who achieved percent-free monocyte $\alpha_5\beta_1$ integrin responses $\leq$1% on weeks 16 were 0.0, 0.2, 11.9, 41.0, 51.0, 58.3, and 74.1%, respectively. This indicates that 10 mg/kg or higher dose is necessary to saturate >95% receptors in majority of patients (>93%).

Discussion

We developed a fully integrated mechanism-based population PK/PD model that described the exposure and monocyte $\alpha_5\beta_1$ integrin-binding relationship in cancer patients treated with volociximab, the first monoclonal IgG_4 antibody

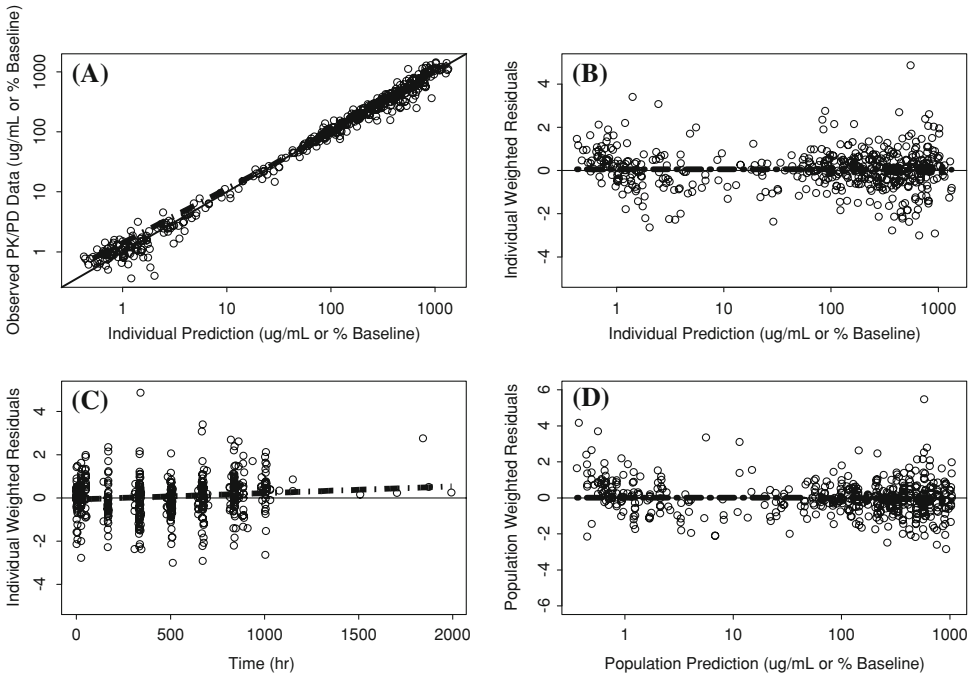

Fig. 4 Model diagnostic plots. **a** individual predicted versus observed PK/PD data **b** individual weighted residual versus individual prediction, **c** individual weighted residual versus time, and **d** population conditional weighted residuals versus population prediction. *Dotted line*, LOESS smoothing line

Table 2 PK/PD parameter estimates from the final model

Parameter	Population mean (%SE)[a]	Interindividual variability[b] (%SE)[a]
CL (mL/h/kg)	0.0544 (21.7)	0.641 (38.5)
CL_d (mL/h/kg)	0.183 (1.7)	–
V_p (mL/kg)	12.5 (22.6)	0.685 (41.7)
V_c (mL/kg)	34.0 (6.2)	0.0749 (32.8)
K_{deg} (h^{-1})	0.00544 (14.3)	0.221 (43.5)
K_{on} (μM/h)	6.61 (26.2)	1.16 (35.7)
K_{off} (h^{-1})	0.000430 (1.4)	–
Baseline (μM)	0.0244 (3.0)	–
θ	0.590 (0.5)	–
σ_{PK}[c]	0.208 (4.2)	–
σ_{PD}[d]	0.432 (6.6)	–

[a] Percent standard error of the parameter estimate = standard error of estimates/parameter estimates ×100%

[b] Interindividual variability is expressed as population variance

[c] Random residual variability of PK model

[d] Random residual variability of PD model; K_{int} was assumed to be equal to K_{deg} in the final model

specifically targeting $\alpha_5\beta_1$ integrin studied in clinical trials. A receptor-binding PK/PD model was developed to quantify the dynamic interaction of volociximab binding to monocyte $\alpha_5\beta_1$ integrin, and this model adequately described the observed clinical data, as illustrated in Figs. 3, 4 and Table 3. To our knowledge, this is the first published population exposure and receptor-binding response model for an anti-integrin antibody in cancer patients.

In the final PK model, the typical V_c (34.0 mL/kg) closely resembles plasma volume, which is expected for a high-molecular weight protein and this is consistent with the values reported for other monoclonal IgG antibodies [8, 21]. The nonspecific clearance (CL) of 0.0544 mL/h/kg represents elimination of volociximab from the central compartment in the absence of receptor-mediated clearance. Consequently, the theoretical typical α and β phase elimination half-life in the absence of receptor-mediated clearance can be calculated using the following equations:

$$t_{1/2\alpha} = \frac{2 \times 0.693}{\left(\frac{CL_d}{V_p} + \frac{CL_d}{V_c} + \frac{CL}{V_c}\right) + \sqrt{\left(\frac{CL_d}{V_p} + \frac{CL_d}{V_c} + \frac{CL}{V_c}\right)^2 - 4\frac{CL_d}{V_p}\frac{CL}{V_c}}} = 1.41 \text{ days}$$

$$t_{1/2\beta} = \frac{2 \times 0.693}{\left(\frac{CL_d}{V_p} + \frac{CL_d}{V_c} + \frac{CL}{V_c}\right) - \sqrt{\left(\frac{CL_d}{V_p} + \frac{CL_d}{V_c} + \frac{CL}{V_c}\right)^2 - 4\frac{CL_d}{V_p}\frac{CL}{V_c}}} = 25.3 \text{ days}$$

These values fall within the range of reported α and β phase elimination half-life of natural IgG_4 in humans [25]. The equilibrium dissociation rate constant for the

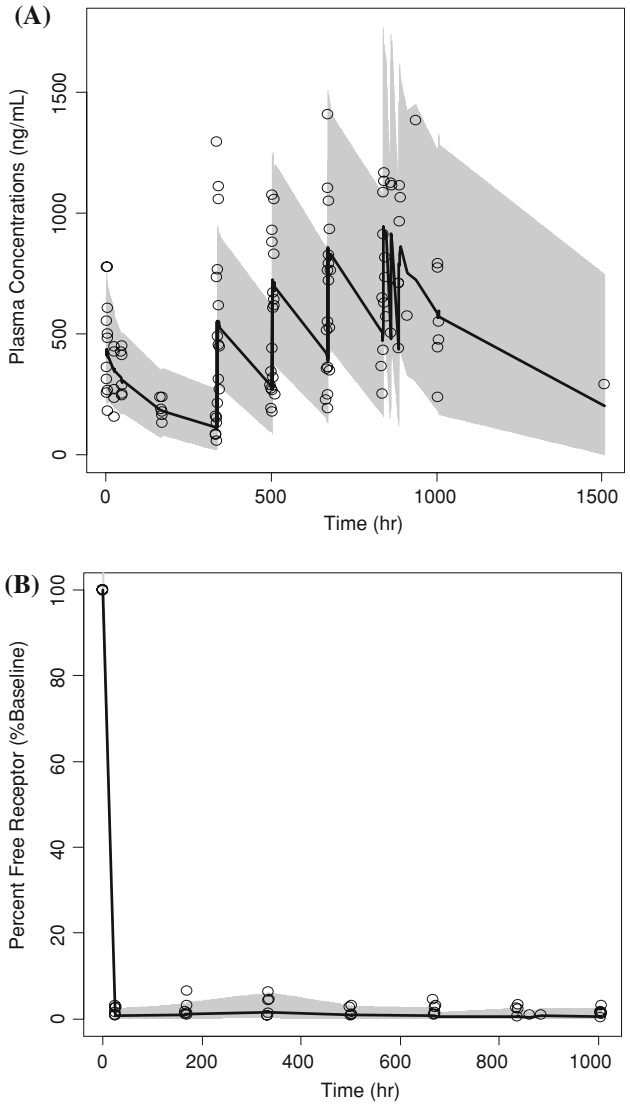

Fig. 5 Visual predictive check of the final PK/PD model for patients who received a dose of 15 mg/kg. *Open circle* observed PK or PD, *solid line* model simulated median values, *shaded area* 90% confidence interval of the simulated values

volociximab-monocyte $\alpha_5\beta_1$ integrin complex K_d calculated as the ratio of K_{off} to K_{on} is estimated as 0.065 nM. This finding differs from the K_d values of 0.37 ± 0.13 nM obtained from in vitro Biacore studies [22]. This discrepancy might be explained by the difference between a closed, controlled microsystem utilized in the in vitro Biacore studies in contrast to the K_d values occurring in an open and dynamic biological system with ongoing disposition of both drug and receptors in cancer patients.

Based on the understanding of the IgG_4 biology and preliminary results from the preclinical studies, volociximab was not thought to induce antibody-dependent cell-mediated cytotoxicity (ADCC) nor complement-dependent cytotoxicity (CDC) (unpublished data; PDL, Inc.). Furthermore, it was initially assumed that the drug–receptor complex was eliminated at the same rate as the free receptor (i.e., $K_{int} = K_{deg}$). During the model development, assigning a different elimination rate constant to free receptor and drug–receptor complex did not significantly improve the model fit ($P > 0.05$). Therefore, the final model assumed that free receptor and drug–receptor complex shared the same elimination pathway. Although the monocyte $\alpha_5\beta_1$ integrin-time profiles following volociximab administration did not reveal rebound phenomenon, the addition of a negative feedback loop on receptor synthesis significantly decreased the objective function (Δ OF = 36, $P < 0.001$) and was incorporated into the final model. More data with long-term follow-up with drug-free period is needed to confirm the presence of the rebound phenomenon. The final receptor-binding PK/PD model is similar to a target-mediated drug disposition model proposed by Mager et al. [19] and to an earlier model we developed to describe the pharmacology of a nondepleting anti-CD4 monoclonal IgG_1 antibody [21]. However, in our current volociximab receptor-binding model, the binding of drug did not alter receptor clearance (i.e., the elimination of free receptor was the same as the elimination of the drug–receptor complex). In addition, our current model expands upon previously reported target-mediated disposition models by incorporating a negative feedback mechanism on the receptor synthesis. Based on the limited PK/PD data used in this study, we have built a PK/PD model based on our current understanding of drug and receptor biology (i.e., drug–receptor binding and no drug-complex internalization) and this model can adequately describe the observed data. The final model consists of 4 PK and 5 PD system parameters. Alternatively, the observed PD data can be described by the indirect model which shared the same number of PD parameters with our model. Indirect model is one of the basic and commonly used PD model, and the differential equations of this model are given in the following:

Table 3 Results of the simplified numerical model predictive check

Percent of observed data	All data	PK data	PD data
Within boundary between 2.5th and 97.5th quantile of simulated set (95% CI)	95.3	95.4	95.2
≥50th (median) quantile of simulated data	49.7	49.1	51.0
<50th (median) quantile of simulated data	50.3	50.9	49.0

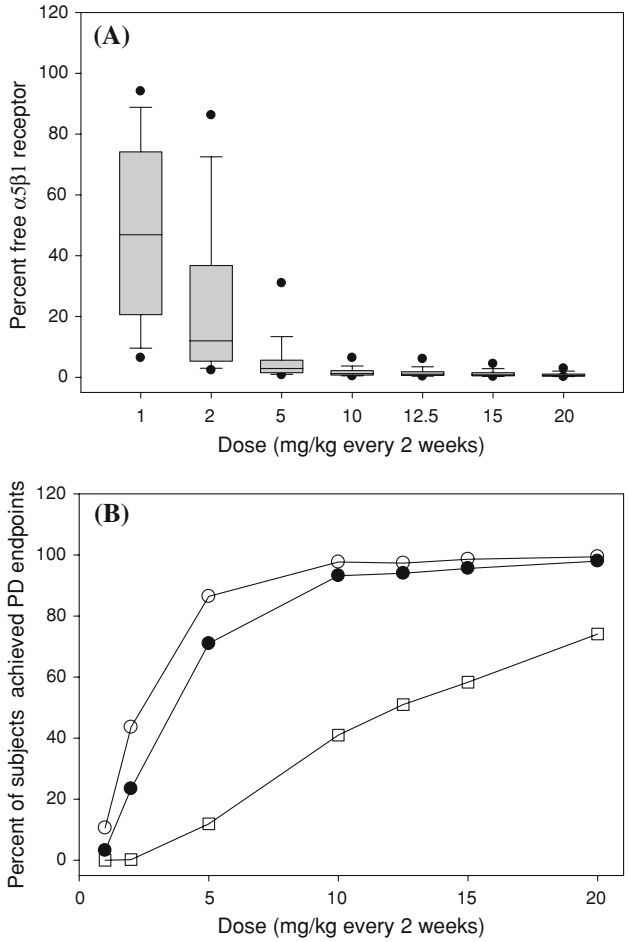

Fig. 6 **a** Distribution of percent-free $\alpha_5\beta_1$ receptor on weeks 16. The *boxes plot* 10th 25th, median, 75th, 90th percentiles and the *dots* are 5th and 95th percentile points, and **b** percent of subjects who had free $\alpha_5\beta_1$ receptor level on weeks 16 less than or equal to 10% (*open circle*), 5% (*solid circle*), and 1% (*open square*) after different dosing regimens of volociximab. Number of simulated subjects 1,000

$$\frac{dR}{dt} = K_{syn} - K_d R\left(1 + \frac{I_{max} C^{\gamma}}{K_m^{\gamma} + C^{\gamma}}\right)$$

where K_{syn} represents zero-order receptor synthesis rate. K_d, I_{max} and K_m represent first-order constant for loss of receptor, maximum effect of drug on free receptor, and drug concentration that achieves 50% effect on drug receptor, respectively. γ is the Hill coefficient. However, we have decided to use the receptor-binding model because it is more closely related to our understanding of the drug and receptor biology. Nevertheless, more data are needed in order to confirm the validity of this model in describing the PK/PD of volociximab in cancer patients.

In order to examine the potential role of the percent-free monocyte $\alpha_5\beta_1$ integrin levels as a biomarker for subsequent clinical studies, multiple dose trial simulations (1,000 subjects/regimen) were conducted using the final PK/PD model to evaluate the percent-free monocyte $\alpha_5\beta_1$ integrin at weeks 8 and 16 after the administration of volociximab at doses of 1, 2, 5, 10, 12.5, 15 mg/kg IV infused over 1 h every 2 weeks. Weeks 8 and 16 were selected because they were potential intermediate clinical endpoints for evaluation in future clinical studies. The simulated percent-free monocyte $\alpha_5\beta_1$ integrin after volociximab administration were similar between weeks 8 and 16, therefore, only the simulation results on week 16 were presented. These simulated results suggest that monocyte $\alpha_5\beta_1$ integrin sites were saturated in the majority of subjects receiving volociximab at doses greater than 5 mg/kg IV every 2 weeks. Assuming that the percent-free monocyte $\alpha_5\beta_1$ integrin level achieving $\leq$5% was used as the criteria for dose selection, then a volociximab dose of 10 mg/kg IV every 2 weeks would be optimal because the receptor saturation dose–response curve plateaued above the 10 mg/kg dose level. Therefore, doses of $\geq$10 mg/kg IV every 2 weeks in the Phase II studies would represent the biologically active dose based on the criteria of achieving a percent-free monocyte $\alpha_5\beta_1$ integrin response $\leq$5%.

The volociximab has been tested at a dose of 10 mg/kg IV every 2 weeks in the Phase II cancer patients with renal cell carcinoma and metastatic adenocarcinoma of the pancreas [9, 27]. However, the information of percent-free monocyte $\alpha_5\beta_1$ integrin was not obtained in those studies. In a multicenter, open label, single cohort, pilot Phase II study, 40 subjects with refractory or relapsed metastatic renal cell carcinoma received volociximab 10 mg/kg IV every 2 weeks monthly until disease progression. Stable disease was observed in 32 (80%) patients including 1 confirmed partial response. Duration of stable disease ranged from 2 to 22 months. Median time for progression was 4 months [27]. In another multicenter Phase II study, 20 subjects with metastatic pancreatic cancer received volociximab 10 mg/kg IV every 2 weeks (days 1 and 15) with gemcitabine 1,000 mg/m^2 IV on days 1, 8, 15, of a 4-week cycle until disease progression. Overall response included 1 confirmed partial response, and stable disease in 10 subjects [9].

However, minimum clinical responses were observed in patients with renal cell carcinoma and metastatic adenocarcinoma of the pancreas, who received a volociximab dose of 10 mg/kg IV every 2 weeks despite the model prediction that a majority of the simulated subjects would have percent-free monocyte $\alpha_5\beta_1$ integrin $\leq$5% at this particular dose. It is possible that while the dose of 10 mg/kg IV every 2 weeks may represent a biologically active dose based on the percent-free monocyte $\alpha_5\beta_1$ integrin levels, it is not a clinically effective dose for cancer patients because the target cells in the tumor may be in the tissue compartment that is less accessible to the drug compared with the monocytes in the well-perfused blood

compartment. Hence, saturation of $\alpha_5\beta_1$ integrin receptors on the monocytes in the blood compartment may not correlate optimally with the receptor saturation on the target cells in tumor, and $\alpha_5\beta_1$ integrin receptor super saturation in circulating monocyte may be necessary to better reflect adequate receptor saturation at the site of action for eliciting desired clinical effects of the drugs. Therefore, the percent of free monocytes $\alpha_5\beta_1$ integrin $\leq 1\%$ ($\geq 99\%$ receptor saturation) after different doses was determined. As illustrated in Fig. 6b, if the goal was to achieve percent-free monocyte $\alpha_5\beta_1$ integrin responses of $\leq 1\%$, then volociximab doses of 10 mg/kg may not be optimal because the percent of subjects achieving this particular endpoint is only 41.0%. At present, whether this degree of monocyte $\alpha_5\beta_1$ integrin receptors saturation is needed for desirable clinical effects is unknown. Traditionally, the relationships between the degree of monocyte $\alpha_5\beta_1$ integrin receptors saturation and the tumor responses can be explored using preclinical xenograft model. However, volociximab and its derivatives do not cross react with mouse and rat $\alpha_5\beta_1$ integrin receptors [22]. Hence, these standard xenograft models are not useful model system for investigating the relationships between the monocyte $\alpha_5\beta_1$ integrin receptors saturation and tumor response. For this reason, the relationships of the degree of monocyte $\alpha_5\beta_1$ integrin receptors saturation with clinical responses would need to be further studied in future clinical studies in order to increase our understanding of the roles of monocyte $\alpha_5\beta_1$ integrin receptors saturation in the anti-cancer effect of volociximab in cancer patients.

In conclusion, a mechanism-based receptor-binding PK/PD model was successfully developed to describe the dynamic interaction between volociximab and monocyte $\alpha_5\beta_1$ integrin binding. The developed model predicted serum volociximab- and percent-free monocyte $\alpha_5\beta_1$ integrin-time profiles quite well. This PK/PD model was used to simulate the percent-free monocyte $\alpha_5\beta_1$ integrin profiles for different volociximab dosing regimens and it provided valuable information for examining the potential role and utility of percent-free monocyte $\alpha_5\beta_1$ integrin as a biomarker in the development of volociximab.

References

1. Bauer RJ, Guzy S (2004) Monte Carlo parametric expectation maximization (MC-PEM) method for analyzing population pharmacokinetic/pharmacodynamic (PK/PD) data. In: D'Argenio DZ (ed) Advanced methods of pharmacokinetic and pharmacodynamic system analysis. Kluwer, Boston, pp 135–163
2. Beal SL (2001) Ways to fit a PK model with some data below the quantification limit. J Pharmacokinet Pharmacodyn 28:481–504
3. Breier G, Risau W (1996) The role of vascular endothelial growth factor in blood vessel formation. Trends Cell Biol 6:454–456
4. Brooks PC, Clark RA, Cheresh DA (1994) Requirement of vascular integrin alpha v beta 3 for angiogenesis. Science 264:569–571
5. Brooks PC, Montgomery AM, Rosenfeld M, Reisfeld RA, Hu T, Klier G, Cheresh DA (1994) Integrin alpha v beta 3 antagonists promote tumor regression by inducing apoptosis of angiogenic blood vessels. Cell 79:1157–1164
6. Cranmer LD, Bedikian AY, Ribas A, O'Day S, Forero-Torres A, Yazji S, Kirkwood M (2006) Phase II study of volociximab (M200), an alpha-5 beta-1 anti-integrin antibody in metastatic melanoma. J Clin Oncol 24:8011
7. D' Argenio D, Schumitzky A (1997) ADAPT II user's guide: pharmacokinetic/pharmacodynamic system analysis software. Biomedical Simulations Resources, Los Angeles
8. Davies B, Morris T (1993) Physiological parameters in laboratory animals and humans. Pharm Res 10:1093–1095
9. Evans T, Ramanathan RK, Yazji S, Glynne-Jones R, Anthoney A, Berlin J, Valle JW (2007) Final results from cohort 1 of a phase II study of volociximab, an anti-alpha5 beta1 integrin antibody, in combination with gemcitabine (GEM) in patients (pts) with metastatic pancreatic cancer (MPC). J Clin Oncol 25:4549
10. Ferrara N, Gerber HP, LeCouter J (2003) The biology of VEGF and its receptors. Nat Med 9:669–676
11. Folkman J (1995) Angiogenesis in cancer, vascular, rheumatoid and other disease. Nat Med 1:27–31
12. Folkman J (2002) Role of angiogenesis in tumor growth and metastasis. Semin Oncol 29:15–18
13. Francis SE, Goh KL, Hodivala-Dilke K, Bader BL, Stark M, Davidson D, Hynes RO (2002) Central roles of alpha5 beta1 integrin and fibronectin in vascular development in mouse embryos and embryoid bodies. Arterioscler Thromb Vasc Biol 22:927–933
14. Friberg LE, Henningsson A, Maas H, Nguyen L, Karlsson MO (2002) Model of chemotherapy-induced myelosuppression with parameter consistency across drugs. J Clin Oncol 20:4713–4721
15. George EL, Georges-Labouesse EN, Patel-King RS, Rayburn H, Hynes RO (1993) Defects in mesoderm, neural tube and vascular development in mouse embryos lacking fibronectin. Development 119:1079–1091
16. Hwang R, Varner J (2004) The role of integrins in tumor angiogenesis. Hematol Oncol Clin North Am 18:991–1006, vii
17. Kim S, Bakre M, Yin H, Varner JA (2002) Inhibition of endothelial cell survival and angiogenesis by protein kinase A. J Clin Invest 110:933–941
18. Kim S, Harris M, Varner JA (2000) Regulation of integrin alpha vbeta 3-mediated endothelial cell migration and angiogenesis by integrin alpha5beta1 and protein kinase A. J Biol Chem 275:33920–33928
19. Mager DE (2006) Target-mediated drug disposition and dynamics. Biochem Pharmacol 72:1–10
20. Ng CM, Joshi A, Dedrick RL, Garovoy MR, Bauer RJ (2005) Pharmacokinetic-pharmacodynamic-efficacy analysis of efalizumab in patients with moderate to severe psoriasis. Pharm Res 22:1088–1100
21. Ng CM, Stefanich E, Anand BS, Fielder PJ, Vaickus L (2006) Pharmacokinetics/pharmacodynamics of nondepleting anti-CD4 monoclonal antibody (TRX1) in healthy human volunteers. Pharm Res 23:95–103
22. Ramakrishnan V, Bhaskar V, Law DA, Wong MH, DuBridge RB, Breinberg D, O'Hara C, Powers DB, Liu G, Grove J, Hevezi P, Cass KM, Watson S, Evangelista F, Powers RA, Finck B, Wills M, Caras I, Fang Y, McDonald D, Johnson D, Murray R, Jeffry U (2006) Preclinical evaluation of an anti-alpha5beta1 integrin antibody as a novel anti-angiogenic agent. J Exp Ther Oncol 5:273–286
23. Ricart AD, Tolcher AW, Liu G, Holen K, Schwartz G, Albertini M, Weiss G, Yazji S, Ng C, Wilding G (2008) Volociximab, a chimeric monoclonal antibody that specifically binds alpha5beta1

integrin: a phase I, pharmacokinetic, and biological correlative study. Clin Cancer Res 14:7924–7929
24. Risau W (1997) Mechanisms of angiogenesis. Nature 386:671–674
25. Waldmann TA, Strober W (1969) Metabolism of immunoglobulins. Prog Allergy 13:1–110
26. Witmer AN, Vrensen GF, Van Noorden CJ, Schlingemann RO (2003) Vascular endothelial growth factors and angiogenesis in eye disease. Prog Retin Eye Res 22:1–29
27. Yazji S, Bukowski R, Kondagunta V, Figlin R (2007) Final results from phase II study of volociximab, an alpha-5 beta-1 anti-integrin antibody, in refractory or relapsed metastatic clear cell renal cell carcinoma (mCCRCC). J Clin Oncol 25:5094